JOURNAL OF PROPULSION AND POWER
Vol. 23, No. 4, July–August 2007

Alternate Direct-Drive Option for Electric Propulsion

Ivana A. Hrbud*
Purdue University, West Lafayette, Indiana 47907

DOI: 10.2514/1.26313

The goal of this research is to power a 1.5-kW Hall thruster with a power source based on chemical double layer capacitor technology and to access performance characteristics of this power/propulsion system. The thruster was operated in a long-pulse mode with decaying power input and exhibited similar performance characteristics to being operated under steady-state conditions. Over the tested power range of 450–1750 W, the thruster generated thrust of 30–100 mN at an efficiency of 30–55% and a specific impulse of 900–1950 s. These results formed the basis for a mission analysis considering extremes with regard to shading and atmospheric density. A near-Earth orbiting spacecraft served as an analysis platform to compare the mission performance of direct-drive electric propulsion options and a state-of-the-art hydrazine monopropellant system. Regardless of orbit conditions, electric propulsion options outperformed the conventional chemical system in terms of wet mass decrease (41–59%) and net mass increase (14–47%), while capacitor-powered electric propulsion options substantially reduced the onboard power requirement (66–91%).

Nomenclature

A	=	area, m^2
C	=	capacitance, F
d	=	thickness of dielectric material, 0.1 nm
E	=	energy, J
e	=	energy density, J/m^3
F	=	electric field strength, V/cm
V	=	voltage, V
ε_r	=	relative dielectric constant
ε_0	=	permittivity of vacuum, $8.854 \cdot 10^{-12}$ F/m
ρ	=	density, kg/m^3

Subscripts

aver	=	average
max	=	maximum
st	=	stored

I. Introduction

COST and spacecraft mass are prominent and driving factors in the exploration of new avenues for spacecraft design. Key elements defining new mission performance characteristics are smaller launch systems, higher launch frequency, new deorbit regulations, reductions of ground operation cost/complexity, and precision positioning for formation flying. For space and Earth exploration in the 21st century it is desirable to achieve cost effectiveness by launching frequently small, low-cost spacecraft. Weight reduction of subsystems such as power source and propulsion systems would yield greater mission payloads and scientific returns in light of space commercialization, science, and exploration missions. Propulsion wet mass can be a substantial portion of a spacecraft. When electric propulsion is considered, the power source/plant is an additional factor. Advancement and progress in the area of thruster and power design play a noteworthy role in reducing spacecraft mass. New technologies incorporated into spacecraft subsystems would increase mission capability and science return, and for selected missions might reduce launch cost due to spacecraft mass improvements.

Since the early 1990s, electric propulsion (EP) has been a vital part of spacecraft propulsion for a wide spectrum of space missions and applications for both industry and government agencies. Commercial satellite manufactures have embraced EP due to significant economic returns. To date, electrothermal (arc- and resistojet), electrostatic (Hall and ion thruster), or electromagnetic (pulsed plasma thruster) systems propel close to 200 spacecraft in various mission scenarios spanning lower Earth orbit (LEO), geostationary/geosynchronous orbit (GST/GSO), and trajectories within the inner planets [1]. An essential subsystem of electric propulsion is the power processing and conditioning unit feeding the thruster to generate kinetic energy. Unlike chemical propulsion, where power source and thrust-producing element are inseparable, electrical energy is delivered, processed, and tailored to the specific needs of the electric propulsion system by a separate unit. Electric power is delivered at voltage/current levels, which are particular to the underlying conversion mechanism. To date the energy drawn through the spacecraft's main power bus for EP comes primarily from solar panels [2,3]. Radioisotope batteries [4–6] or a nuclear fission reactor [7,8] are viable options and have been considered in numerous studies; however, these power source/plant alternatives have not been implemented beyond the research and development phase.

Because of a wide scope of mission scenarios envisioned by both industry and government agencies, some future spacecraft will be severely power-limited [9] and the use of power-consuming electric thrusters is questionable. For continuous operation power consumption of EP devices, which were typically implemented on spacecraft since the mid-1990s, is greater than 500 W per thruster. Another limiting factor of conventional spacecraft design and architecture is mass and volume, which ultimately are dictated by part count and complexity. Particular components within the powertrain condition the power (provided at the spacecraft power bus) to thruster-specific operating requirements (voltage/current). Complexity and part count of an EP powertrain, and ultimately mass and volume of the EP system, could be potentially reduced when power conditioning and processing are reduced to a minimum or completely eliminated. One such option arose with the development of high-voltage solar arrays, which enable direct-drive operation of Hall and ion thrusters [10,11]. Potential limiting factors with regard to this option are high cost and potential space environment effects (e.g., high-voltage surface breakdown) [12], not necessarily acceptable to the spacecraft manufacturer.

Another direct-drive concept considers a high-energy density and high-power density capacitor bank for intermediate energy storage.

Received 3 July 2006; revision received 23 January 2007; accepted for publication 25 January 2007.

*Assistant Professor, School of Aeronautics and Astronautics, 315 North Grant Street. Member AIAA.

These unique performance characteristics are provided by chemical double layer (CDL) capacitor technology. Low average power provided by the power source (i.e., solar arrays) is stored in the capacitor bank and later used at power levels required/dictated by the employed EP thruster. It enables long-pulse operation of an electrostatic thruster with conventional solar arrays and minimal control/interface circuitry, thus also reducing the need for power conditioning and processing. Such an electric propulsion system allows "minutes" of high-power and high-efficiency propulsion to the spacecraft. The pulse repetition rate determines the average power necessary to perform the desired maneuver. This allows small, low-power spacecraft to employ the advantages of high-power, high-efficiency thrusters without producing excessive demands on the spacecraft's powertrain.

This paper summarizes experimental performance characteristics of a Hall thruster powered with a CDL capacitor bank in a direct-drive configuration. The main objective of the research was to demonstrate and validate an alternative direct-drive option that reduces cost, complexity, part count, mass, volume, and power demand. The paper does not intend to weight the different powertrain options, but mainly tries to showcase a viable alternative and its potential benefits to mainstream powertrain architecture. A brief overview of CDL capacitor technology is provided to introduce the reader with the specific characteristics of this energy storage medium. The paper concludes with a preliminary assessment for potential applications for near-Earth orbits.

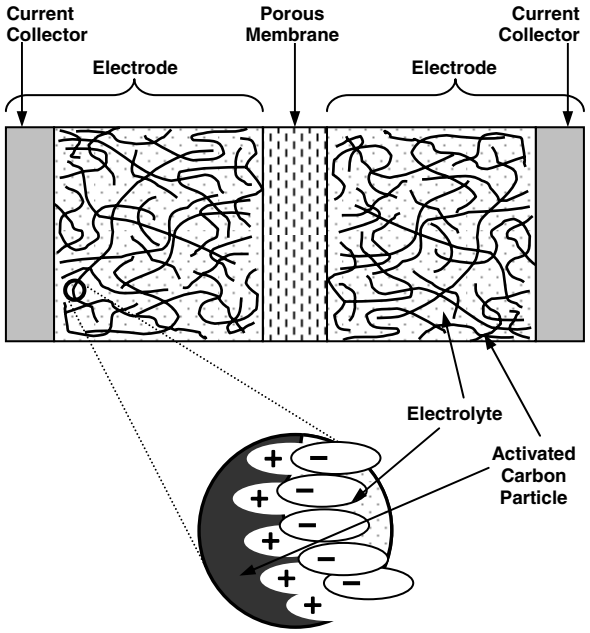

Fig. 1 CDL capacitor structure and microscopic chemical double layer.

II. CDL Capacitor Technology

Research of chemical double layers dates back the middle of 19th century. In 1853, von Helmholtz [13] formulated the first model for double layers. Since the discovery, researchers advanced and refined the theoretical description by considering specific adsorption and physical nature of the boundary region between the substances [14]. Chemical double layers have a wide application spectrum [15]. In one such application, double-layer capacitors have been tested in the laboratory to provide peak power for thrust vector control actuation [16] on the Space Shuttle's solid rocket motors. In recent years, chemical double layers have received significant attention for energy storage and capacitor development. Their advancement depends strongly on the science of the solid–liquid interface [17].

Two conducting plates (electrodes) separated by an insulator (dielectric) form the most basic capacitor. In 1879, von Helmholtz discovered that the interface between a conductor and a liquid electrolyte formed a layer capable of storing charge [18]. Negative and positive charges align on the interface between the conductor and the electrolyte. The boundary area between these charges is the electrical double layer. Figure 1 shows both the microscopic electric double layer and the principle structure of a CDL capacitor. The electrode of a unit cell is made of activated carbon particles or fibers with large surface area. The electrode is bonded to a thin metal foil (e.g., aluminum, gold, etc.) that functions as the current collector and the entire electrode is impregnated with an aqueous or organic electrolyte solution. A porous membrane separates two electrodes. This separator possesses high insulation properties against electrons, while it permits conduction of ions. Materials such as carbon allow large capacitance-to-volume ratios [19,20].

The electrolyte solution primarily dictates the operating condition of this type of capacitors. Aqueous electrolytes (e.g., potassium hydroxide, sulfuric acid) offer high-power densities and low internal resistance. However, such chemical solutions are corrosive and are not suitable for applications with long life requirements. Organic electrolytes operate at higher voltages, which impart higher energy densities than aqueous electrolytes. However, high internal resistances limit the application range for capacitors based on this electrolyte [19].

Capacitance ($C = \varepsilon_0 \varepsilon_r A/d$), stored energy ($E_{st} = 0.5CV^2$), and energy density ($e = 0.5\varepsilon_0 \varepsilon_r F^2$) are main capacitor properties. Increasing either the capacitance or the breakdown strength of the storage media will yield higher storage density. Dielectric constant and voltage at which the layer fails are strong functions of the electrolyte species and their concentration. Focus areas of CDL capacitor research are area-to-thickness ratio, breakdown voltage of the interface, formation of large surface areas [19,20] (activated carbon), and identification of materials with low resistance (ruthenium oxides) [21,22].

In the past, batteries and electrolytic capacitors have dominated energy storage systems in pulsed applications. Although batteries possess high-energy densities relative to CDL capacitors, they suffer from low-power densities and have poor charge–discharge cycle ability. Electrolytic capacitors achieve moderately high energy and power densities, but are sensitive to polarity, thermal effects, and discharge rate. Energy density of CDL capacitors is five times greater than that of electrolytic capacitors, whereas power density of CDL capacitors is at least an order of magnitude higher than that of batteries [23,24]. CDL capacitors outperform conventional rechargeable batteries in the number of charge–discharge cycles with minimal degradation, even if the charge voltage is 30% higher than the manufacturer's specifications [25].

CDL capacitors exhibit favorable volume-to-mass ratios and fabrication flexibility with regard to shape. These attributes might be valuable in meeting future packing and subsystem integration needs. Table 1 summarizes available power storage technologies and their characteristics for space applications.

III. Apparatus and Experiment

The main objective of this research is to experimentally validate an alternate direct-drive configuration for electric propulsion, which provides significant reduction in spacecraft complexity. Figure 2 illustrates block diagrams for conventional and alternative powertrain configurations. The top block diagram depicts the most commonly used powertrain (encompassing conventional solar-array technology, power conditioning, and processing unit) in laboratory

Table 1 Comparison of available power storage technologies for space applications

Characteristics	CDL capacitor	Electrolytic capacitor	Battery
Energy density, kJ/kg	10–20	1–2	500
Power density, kW/kg	5–10	1–3	<0.05
Life	Long	Moderate	Moderate
Cycle ability	Extremely high	Moderate	Low

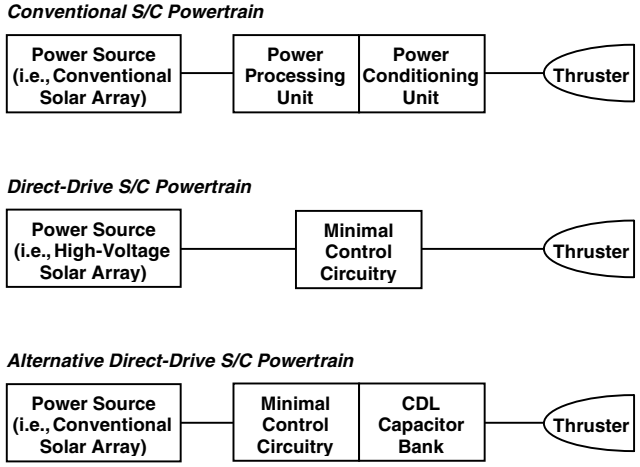

Fig. 2 Conventional and alternative powertrain configurations for EP.

[26,27] and flight settings. Significant solar-array technology advancement and development of high-voltage solar array enable the direct-drive option depicted in the middle block diagram. In this option a Hall or an ion thruster are powered directly of the high-voltage solar array requiring minimal control circuitry. The last block diagram outlines the powertrain of an alternate direct-drive option using the CDL capacitor bank as intermediate energy storage, conventional solar-array technology for charging the bank, and minimal control circuitry.

The main feature of this direct-drive configuration is the elimination of power processing and conditioning units commonly used in conventional electric propulsion powertrains. Operating conditions of this configuration target an average power of 1500 W and discharge voltages of 200–400 V. To satisfy these electrical requirements, a Hall thruster was chosen for experimental testing with the alternate direct-drive option. In particular, the Hall thruster is the Russian D-55 thruster with anode layer (TAL) operating on xenon. The model classification "D-55" refers to the inner diameter (in millimeters) of the annular discharge chamber. Previous investigations [26,28] report a specific impulse of 1600 s and an efficiency of 48% at a nominal operating power level of 1300 W and a discharge voltage of 300 V. These studies were performed with a conventional powertrain configuration. The discharge current is determined by the anode mass flow rate and at a specific setting remains essentially constant for a wide range of discharge voltage [26]. However, the current increases exponentially below a certain voltage threshold, which is dictated by the magnetic field strength. The optimum magnetic field strength corresponds to a minimum in the discharge current, which in turn signifies a maximum in thruster efficiency [26]. For any magnetic field strength setting, a linear relationship between anode mass flow rate and current exists above that voltage threshold. Thrust is directly proportional to increasing voltage for each anode mass flow rate (i.e., current). The operation principles of the thruster and hollow cathode are discussed elsewhere [29]. The following sections describe the powertrain components of the direct-drive configuration, facilities, and diagnostics.

A. CDL Capacitor Power Source

The CDL capacitor power source consisted of a capacitor bank, charging/discharging power supply, and associated circuitry. Figure 3 illustrates the circuit schematic of the powertrain that was

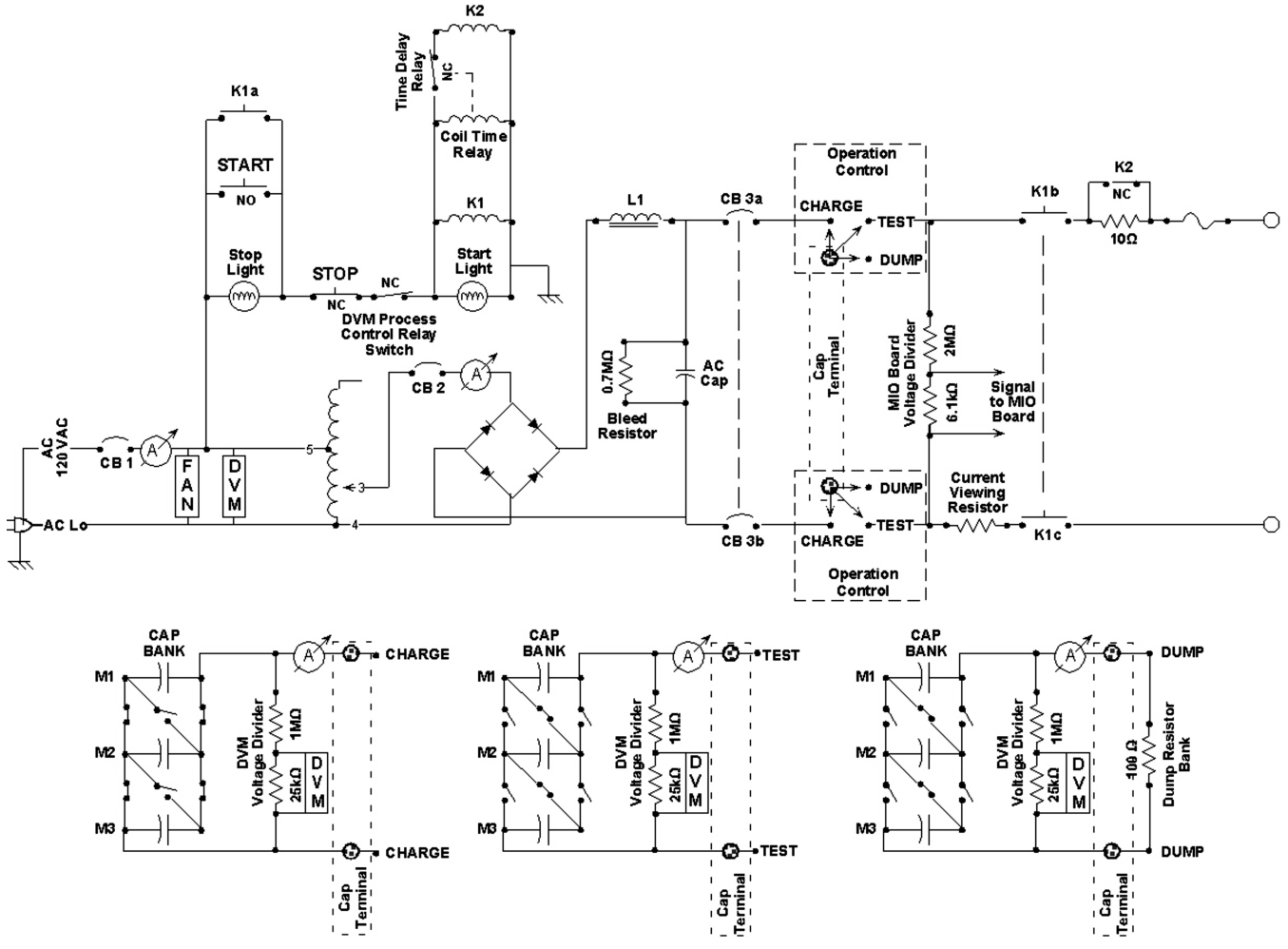

Fig. 3 Circuit schematic of powertrain used in experiments.

used in the laboratory for this investigation. The capacitor bank was designed and configured to meet the specifications of the D-55 TAL. The capacitor bank contained Panasonic CDL capacitors each rated 470 F at a nominal operating voltage of 2.3 V. For each capacitor, a simple test determined the equivalent series resistance (ESR) and capacitance at a charge voltage of 3 V [30]. The capacitor bank consisted of 135 units wired in series, which were distributed on three arrays of 45 units each. Each array denotes a capacitive stage (M1, M2, M3) in the capacitor bank. Based on an average unit capacitance of 540 F, the total capacitance of the bank was 4 F and the designed operating voltage was 400 V. This resulted in an overall energy storage capacity of 320 kJ and a total bank ESR of approximately 800 mΩ (based on an average unit ESR of 6 mΩ).

The capacitor bank was based on the Marx bank concept invented in the early 1920s [31]. Operational principle is based on configuring a series of capacitive stages in parallel for charging at low voltage and achieving voltage multiplication by switching these stages in series for discharging at high voltage. As mentioned earlier, the CDL capacitor bank consisted of three stages, each charged in parallel configuration to a voltage of about 135 V. On configuring the stages in series, the bank had an operation voltage of approximately 405 V. Because a final output switch was used to connect the bank to the thruster, erecting the Marx bank (voltage increase) occurred without stress on the stage-configuring switch (parallel vs series configuration of stages). Similarly, the switch was opened when the charge on the capacitors comprising the Marx bank was discharged. As a result, the switch was not subjected to any arc erosion. In addition, using this technique resulted in significantly shorter charging periods, which was about 5 min vs 30 min for charging in series all 135 capacitors. The powertrain simplification and reduced part count are the major advantages of using the Marx bank concept.

The charging/discharging power supply was specifically designed to quickly charge the CDL capacitor bank to a maximum voltage of 400 V and included power electronics to facilitate controlled, direct discharging of the stored energy into the TAL. The power supply was designed for a residential 120 VAC/15 A receptacle eliminating special input power requirements. Further, it featured charge/discharge-monitoring devices, current limiting start sequence circuits, and switches for stage (parallel/series) configuration and operation (charging/testing/dumping) control.

B. Facilities and Diagnostics

Testing of the direct-drive concept and the D-55 TAL was conducted in a stainless steel vacuum chamber. The vessel has a diameter of 1.5 m and is 4.6 m long. Four oil diffusion pumps rated at pumping speeds of 30,000 l/s each provided a vacuum pressure between 5 and 9×10^{-5} Torr during thruster operation. Ion gauges monitored vacuum chamber pressures at two locations: one was located about the exit plane of the thruster, whereas the other was about 2 m further downstream. The thruster was mounted on an inverted pendulum-type thrust stand [32], which positioned the thruster along the centerline of the vacuum chamber. Isolated power supplies powered thruster subsystems such as cathode keeper, heater, and magnets [33]. The thruster used xenon as propellant. The anode and cathode propellant flow rates were regulated by 100-sccm and 20-sccm thermal-conductivity flow controllers, respectively. A constant volume technique was applied for the calibration of the controllers [26,30].

LabVIEW provided data acquisition and logging of thrust stand deflection, discharge voltage, and current. A digitizing oscilloscope provided backup diagnostics for voltage and current waveforms, while a strip-chart recorder recorded thrust stand deflections as a function of time. In addition, the thruster operator monitored (real-time) discharge current and cathode-to-ground voltage with two isolated digital multimeters having an input impedance of 10 mΩ. The charging/discharging power supply incorporated a voltage divider and current viewing resistor for measuring discharge voltage (between anode and cathode) and discharge current, respectively.

Table 2 Summary of power supply settings for TAL subsystems

Subsystem	Voltage, V	Current, A	Power, W
Inner magnet	7.5	4.2	31.5
Outer magnet	3.5	1.0	3.5
Cathode keeper	10.3	0.35	3.6
Heater	10.5	8.0	84.0

C. Experimental Procedure

The power supplies for magnets, keeper, and heater were adjusted to specific values and were not changed during the entire testing process. Table 2 summarizes these power supply settings for the TAL subsystems.

Calibration of the thrust stand was performed in situ before and after test runs by loading the apparatus with precisely calibrated weights. The anode/cathode propellant flows were turned off during the calibration procedure. The thruster's magnetic fields had no effect on thrust stand calibration or actual thrust measurements [26,27]. After analyzing all calibration sequences, the zero drift (offset of zero point before and after test series) for this thrust stand is 0.27% or 0.32 mN of the full-scale deflection. Similarly, hysteresis attributed less than 0.3% (0.35 mN). In conclusion, a conservative uncertainty for thrust-stand measurements is within 0.5%. Thermal-conductivity flow controllers adjusted the xenon flow rates through the anode and cathode. A constant-volume technique was applied to calibrate the flow controllers. The uncertainty for anode and cathode mass flow was $\pm 1\%$ after taking into account constant volume, pressure, temperature, and time readings. The propellant flow rate through the cathode was set to 0.59 mg/s and was held constant throughout the testing. The anode propellant flow rate ranged from 3 to 4.6 mg/s and test data was recorded in increments of 0.25 mg/s. This resulted in a total of seven different mass flow settings. To substantiate and verify results, each setting was run twice at an initial discharge voltage of 400 V. In addition, four mass flow settings were selected, at which the thruster was run from an initial discharge voltage of 300 V. This process enabled performance evaluation and repeatability verification at lower voltage. The CDL capacitor bank provided the main energy for the discharge between the anode and cathode. The current through the thruster, and thus the discharge power rate, was controlled by the set anode mass flow rate. A 10 mΩ ballast resistor limited the inrush current during the startup sequence. Then 500 ms into the test cycle, a time-delay relay shorted out (across) the ballast resistor. When the discharge voltage reached 150 V, the power supply was turned off, thus completing the test cycle. The CDL capacitor bank was then recharged for the next test cycle.

IV. Experimental Results

The 4-F CDL capacitor bank stores 320 kJ when charged to its design voltage of 400 V (180 kJ at 300 V). As energy is depleted from the capacitor bank, the voltage across the capacitor bank decreases. Hence, the thruster operates minutes at a time before the capacitor bank has to be recharged. How fast the energy is removed depends on the current at which the experiment is operated. In other words, the higher the current is, the faster the stored energy is depleted, and consequently the thruster operates for shorter periods of time. As discussed in an earlier section, the current in a Hall thruster will only depend on the anode mass flow rate. Anode mass flow rates varied from 3 to 4.6 mg/s and were changed in increments of 0.25 mg/s. Another consequence of the decreasing bank voltage is that thrust and all other resulting performance parameters are functions of time. To maintain clarity, diagrams in this section reflect experimental results/data achieved at the lowest and highest mass flow setting (i.e., 3.04 and 4.57 mg/s). Experimental data for the other five mass flow settings fall between the lower and upper limit [30]. Specific impulse and efficiency were calculated using total mass flow rates (anode plus cathode mass flow rate). Because of the nature of the experiment, the thruster operates minutes at a time. As discussed earlier, uncertainties for the thrust measurement and mass flow rate adjustments are less

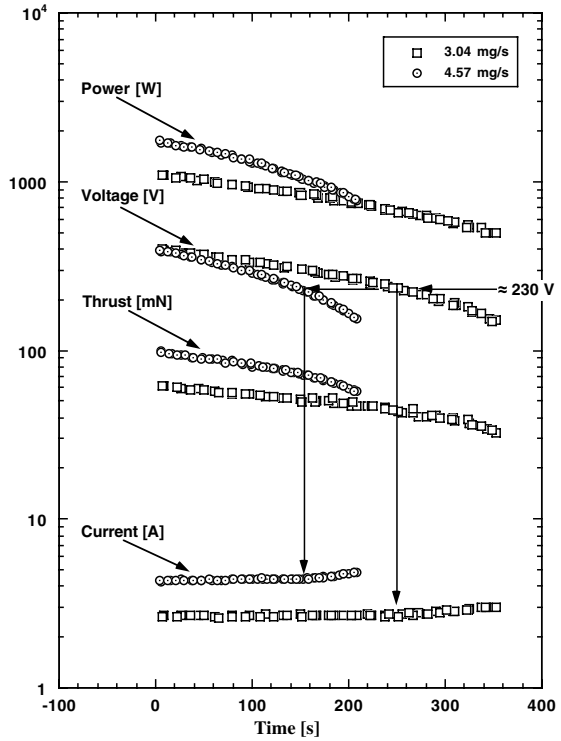

Fig. 4 Voltage, current, power, and thrust as a function of time and anode mass flow rate.

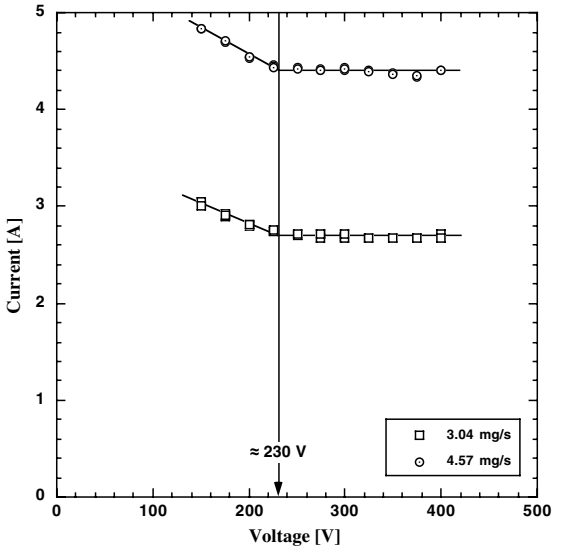

Fig. 5 Current as a function of voltage and anode mass flow rate.

than 0.5% and ±1%, respectively. Because of the logarithmic nature of the data representation, sample error bars are not included.

Russian Hall thruster technology, namely, stationary plasma thruster (SPT) and TAL, has been extensively investigated since its introduction to the United States in the 1990s. Sankovic et al. have authored several reports on operation and performance characteristics of Hall thrusters that were operated with conventional powertrain configuration [26,27]. A qualitative comparison of this study with results reported by Sankovic and Haag [26] show equivalent performance characteristics and trends; however, differences in the experimental setup (i.e., steady-state vs long-pulse operation, vacuum chamber) and, more importantly, the use of different cathode technologies does not allow a quantitative comparison of the two studies.

Figure 4 reflects the time-dependent nature of this experiment by providing the measured values of voltage, current, power, and thrust as a function of time and anode mass flow rate. At least two tests runs were performed for each mass flow rate. These individual test runs are not differentiated in the presentation of the data. The apparent higher density of data towards the end of each test stems from test runs conducted at lower discharge voltage (300 V). All test cases exhibit excellent reproducibility.

As expected, voltage decreases with time at a rate dictated by the rate at which charge is depleted from the capacitor bank, that is, current. The distinct slopes of the voltage waveforms represent this dissipation, which is steeper at higher currents. Consequently, the resulting operating time of the thruster (pulse length) depends on current (anode mass flow rate) and stored energy (charge voltage for a given capacitor). For the present experiments, pulse lengths varied between 210 s (4.57 mg/s) and 350 s (3.04 mg/s). Each test was terminated at about 150 V as recommended by Sankovic [26]. At that voltage, the remaining energy stored in the CDL capacitor bank was about 14% of its initial value at 400 V (320 kJ).

For TAL operation, anode mass flow rate controls the discharge current, which is independent of voltage input (constant/varying). Discharge current is proportional to anode mass flow rate. The chosen range for anode mass flow rates (3.04–4.57 mg/s) produced currents between 2.7 and 4.35 A. Figure 5 illustrates current as a function of voltage and anode mass flow for the magnetic field set by the values in Table 2. In line with the operational principle of a TAL, current is constant over time and only depends on the anode mass flow rate. As reported, this behavior is valid within a particular voltage range, which in turn is dictated by the magnetic field strength [26]. The current remains constant until voltage drops to a characteristic value of about 230 V then increases as the voltage continues to drop.

The thrust of a propulsion system depends on the mass flow rate and the exit velocity of the propellant. Mass flow rates were set and remained constant during individual tests. A TAL uses electrostatic fields to accelerate charged particles (ions). As the acceleration voltage decays with time, momentum change exerted on ions decreases, generating less thrust. Although exit velocity is a strong function of acceleration voltage (400 decaying to 150 V for all tests), higher mass flow rates achieve higher thrust, which is available for shorter pulse lengths. Thrust ranges from 32 to 98 mN depending on mass flow rate and time.

Figure 6 shows thrust, specific impulse, and efficiency as a function of power and anode mass flow rate. As already noted, thrust

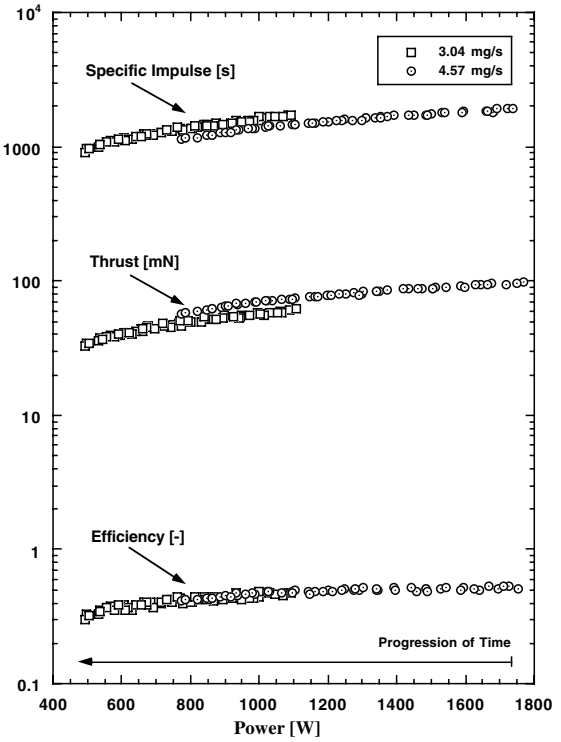

Fig. 6 Thrust, specific impulse, efficiency as a function of power and anode mass flow rate.

increases with increasing anode mass flow rate at given power levels. Thus, higher thrust is achieved at the expense of acceleration voltage. For all tests, thrust at the end of a test drops to about 70% of its initial value. The pulse length for 4.57 mg/s is about 40% shorter than for 3.04 mg/s. Thrust decreases linearly with decreasing power.

The highest specific impulse at a given power level occurs at the lowest mass flow rate. Increasing voltage and decreasing current contribute to higher specific impulse in all cases. Overall, the specific impulse covers a range between 900 and 1950 s depending on anode mass flow rate and time. With increasing power input, efficiency approaches asymptotically a value of approximately 53%. High efficiencies are achieved with greater propellant mass flow rates and power inputs.

V. Mission Analysis

A. Definition of Mission Analysis

The primary goal of the mission analysis is to provide a preliminary assessment of performance for direct-drive electric propulsion options as compared to a state-of-the-art (SOA) hydrazine monopropellant system [34]. The Ozone Research with Advanced Cooperative Lidar Experiments (ORACLE) spacecraft [35,36] serves as an analysis platform to determine the propulsion system's ability of producing the required Δv and compensating drag (offsetting drag) in low-Earth orbit (LEO). The spacecraft has an initial mass of 1000 kg and a projected area of 5 m^2, not including solar arrays. A 600-W solar array powers the payload of the spacecraft. None of its power is allocated to the propulsion system. The objective is to keep the spacecraft in a 300-km, sun-synchronous orbit for two years within a $\pm$1-km operational band. The heliosynchronous orbits, considered for this analysis, are the dawn/dusk (D/D) and noon/midnight (N/M) orbits, which present very different drag compensation scenarios for a spacecraft. In both cases, the solar panels are always oriented towards and perpendicular to the sun. Consequently, the solar array causes negligible drag during the dawn/dusk orbit, because the solar array is parallel to the velocity vector. For the noon/midnight orbit, the solar array is perpendicular to the velocity vector and thus produces significant drag. The analysis assumes that drag (produced by half of the solar-array area) during the noon/midnight orbit is present at all times. To account for the fluctuations in the atmosphere, the mission analysis accounts for a solar (all-time) average (ρ_{aver}) and maximum atmospheric density (ρ_{max}). The other significant difference between these two orbits is the amount of shading experienced by the solar arrays during one revolution. The solar arrays are exposed to the sun for about 60% during the noon/midnight orbit, whereas the dawn/dusk orbit imparts no shading on the spacecraft. Assuming constant drag, the mission analysis used a simple iterative routine to calculate the change of orbit altitude vs thrust over a circular orbit. The thrust pointed into the tangential direction at all times during firing.

The target characteristics of the mission analysis are available net mass, two-year system wet mass, and electric propulsion power requirements. In particular, increase of available net mass and reduction of both system wet mass and EP power requirements are desirable. Wet mass is defined as the mass of all components attributed to the propulsion system. Net mass is usable spacecraft mass analogous to the payload of a spacecraft in orbit. Other output parameters encompass burn time per charge, duty cycle, capacitor charge time, power for charging capacitors, and solar-array mass for EP [37]. Duty cycle is defined as thruster burn time vs total time, whereas total time signifies the combined time the spacecraft transverses the 2-km orbit band (301–299 km) due to drag and then is raised back to its starting position (301 km) due to thrust.

B. Power System Options

Solar arrays based on Gallium Arsenide (GaAs) technology supply energy to either recharge a CDL capacitor bank or to power a Hall thruster via a power processing unit (PPU). The GaAs solar arrays yield 224 W/m^2 and have a mass-to-power ratio of 53 kg/kW. The size of solar arrays (i.e., power needed) for the capacitor direct-drive (Cap-DD) system is an output parameter of the mission analysis and is added to the existing 600-W payload solar array. The analysis tailors the size of the solar arrays such as to provide sufficient energy for charging the capacitor bank. In turn, the capacitor bank supplies then on average 1200 W to operate the Hall thruster. The solar-array-driven (SA) system adds about 5.36 m^2 and 63.6 kg to the existing solar array (payload) to supply the required energy for the Hall thruster. The PPU between the thruster and solar array has an efficiency of 92% and a specific power of 0.1 kW/kg.

The mission analysis considers two capacitor banks. One bank is based on the Panasonic CDL (Pan) capacitors as tested with the D-55 TAL. The other bank consists of experimental CDL capacitors (under development) and is designated "Max." The two technologies differ significantly in key capacitor parameters namely, capacitance, ESR, mass, and volume. A conservative efficiency of 98% is assumed for both capacitor banks. The necessary switching/network circuitry has a specific power of 1 kW/kg. Because thruster operation is terminated at 150 V, the thruster dissipates about 86% of the stored energy, which is replenished during the charging period. CDL capacitors can endure an extremely high number of charge/discharge cycles with minimal degradation, which exceeds the capability of Hall thruster cathodes limited to about 30,000 restart cycles. To take into account the cathode lifetime, the analysis adds capacitor banks if needed to enable longer thruster burn times for each firing. Table 3 lists power parameters and resulting propulsion system characteristics, whereas Table 4 summarizes all significant capacitor bank parameters necessary for the mission analysis.

Table 3 Summary of propulsion system characteristics

Characteristics	Cap-DD	SA	SOA
Thruster characteristics			
Specific impulse, s	1400	1400	225
Thruster efficiency	55%	55%	——
Thruster mass, kg	8	8	0.33
Propellant system mass, kg	1	1	1.82
Propellant tankage fraction	0.100	0.100	0.072
Propellant density, g/cm^3	1.71	1.71	1.00
Power system characteristics			
GaAs SA mass, kg	DIA[a]	63.6	——
GaAs SA area, m^2	DIA	5.36	——
SA power, W	DIA	1200	——
Power source output, W	1200	1200	——
PPU mass, kg/kW	1	10	——
PPU efficiency	98%	92%	——
Propulsion system characteristics			
Number of thrusters	1	1	2
Overall efficiency	54%	51%	——
Total engine thrust, mN	95	88	4.45 N
Total mass flow, mg/s	6.9	6.4	2 g/s

[a]DIA = determined in analysis

Table 4 Summary of capacitor bank specifications

Specification	Pan	Max
Charge voltage, V	405	378
Capacitance, F	4	25.7
ESR, Ω	0.81	0.13
Stored energy at charge voltage, kJ	320	1836
Mass, kg	40.5	61
Capacitance/volume, mF/cm^3	0.08	0.7
Energy/mass, J/g	7.9	30.1

C. Propulsion Options

The mission analysis compares the performance of two EP-propelled options with a SOA hydrazine monopropellant system (SOA). SOA thruster provides the baseline for comparison and is characterized by a specific impulse of 225 s and a thrust of 2.225 N. When operating a Hall thruster with a capacitor bank, the voltage

drops from a designated upper (400 V) to a lower limit (150 V). As demonstrated in the preceding experiments, this voltage variation causes a variation in thruster performance, namely, thrust, specific impulse, and efficiency. For the purpose of this study, average performance points were chosen, which are also employed for the solar-array-powered system. This creates similar thrust performance and fuel consumption, but highlights clearly the impact of the power system. Both EP-propelled systems consider a Hall thruster delivering a specific impulse of 1400 s and an efficiency of 55% at approximately 1200 W. Table 3 summarizes thruster characteristics used in this analysis.

D. Results of Mission Analysis

The objective of the mission analysis was to assess mass and power (i.e., cost) benefits to the ORACLE spacecraft when propelled by Hall thrusters. The chosen orbits (no shading vs maximum shading) and atmospheric densities (solar average vs solar maximum) bound the problem to specific extremes (total of four conditions) and imposed a defined impact on drag in LEO. In general, all three EP options kept the ORACLE spacecraft in the desired orbit regardless of the imposed extreme (condition). Table 5 provides a comprehensive summary of significant mission analysis results.

There were significant improvements with regard to wet mass decrease and net mass increase for each of the four cases (combining shading and atmospheric density). For all four cases, EP options outperformed the baseline with regard to wet mass requirements, which translates into significant savings. The wet mass decrease of the spacecraft was as little as 41% (for Pan-DD, N/M, ρ_{max}) and reached as high as 59% (for SA and Max-DD, D/D, ρ_{max}). Among each other, the EP options exhibit comparable performance for any given case. As expected, the dawn/dusk orbit with average atmospheric density imposed the least drag compensation requirements on the propulsion systems. Consequently, this scenario produced the smallest amount of improvements with regard to net mass increase as compared to the baseline. Overall, net mass increase spanned a range from 14 to 47%.

Table 5 Comprehensive summary of mission analysis results

EP option	D/D ρ_{aver}	D/D ρ_{max}	N/M ρ_{aver}	N/M ρ_{max}
WET mass decrease to SOA, %				
SA	45.7	59.1	44.4	51.3
Pan-DD	58.1	54.1	43.7	40.8
Max-DD	49.1	59.1	50.1	55.2
NET mass increase to SOA, %				
SA	14	39.9	17.6	43.4
Pan-DD	17.8	36.5	17.3	34.5
Max-DD	15	39.9	20	46.7
Power requirements, W				
SA	1,200	1,200	1,200	1,200
Pan-DD	111	222	252	519
Max-DD	111	222	252	409
Number of capacitor banks				
SA	——	——	——	——
Pan-DD	1	2	2	3
Max-DD	1	1	1	1
Duty cycle				
SA	0.1	0.19	0.17	0.33
Pan-DD	0.09	0.18	0.12	0.24
Max-DD	0.09	0.18	0.12	0.24
Thruster burn time, min				
SA	288	288	576	864
Pan-DD	3.8	7.6	7.6	11.5
Max-DD	21.9	21.9	21.9	21.9
Capacitor charge time, min				
SA	——	——	——	——
Pan-DD	43.3	43.3	38.2	27.8
Max-DD	248.6	124.3	109.7	67.6
Number of thruster burn cycles				
SA	375	726	553	645
Pan-DD	22,297	20,625	22,918	26,738
Max-DD	3,886	7,190	7,989	11,736

Power from the solar arrays is available always during the dawn/dusk orbit and only 60% of the time for the noon/midnight orbit. Regardless of the shading/density combination, the SA-powered EP system requires a 1200-W solar array (5.4 m^2, 64 kg). Both Cap-powered EP options provide significant savings regarding solar arrays, which directly translates in mass, area, and, most importantly, cost savings. The capacitor systems require as little as 111 W (0.5 m^2, 5.9 kg) of dedicated solar array for D/D–ρ_{aver} and no more than 409 W (Max-DD, 1.8 m^2, 21.7 kg) and 519 W (Pan-DD, 2.3 m^2, 27.5 kg) for N/M–ρ_{max}, respectively.

The presence of a (large) solar array is most evident for the noon/midnight orbit, where a large solar array will cause a significant amount of drag. The solar array of the SA-powered option will degrade the orbit of the spacecraft more rapidly, which in turn will impose more frequent raising of the orbit altitude. Consequently, the duty cycle for the considered extremes of atmospheric density is 17 and 33%. Capacitor-powered EP options for these two cases exhibit an advantage of 5 (ρ_{aver}) to 9 (ρ_{max}) percentage points. For the minimum shade orbit, all EP options have comparable duty cycles regardless of atmospheric density. The orientation of the solar array with respect to the velocity vector causes negligible drag. The size of the solar array is not a factor and drag is only a function of the spacecraft's projected area.

The SA-powered EP option has a clear advantage with regard to thruster burn cycles. The Pan-DD option imposes the most number of thruster burn cycles (20,625–26,738). With increasing demands on orbit maintenance, this option requires additional capacitor banks to keep that number below the stipulated 30,000 mark. Because of superior capacitance-to-volume and energy-to-mass ratios, the Max-DD option outperforms the Pan-DD option with regard to thruster burn cycles. In addition, it does not require additional capacitor banks to provide essentially the same duty cycle.

VI. Conclusions

The main objectives of this research set out to experimentally evaluate performance and demonstrate an alternate direct-drive concept for a Hall thruster (TAL-D55) using a unique power source. To substantiate the study further, a near-Earth orbit was chosen to showcase a preliminary assessment for a potential application. Special attention during this study was given to cost reduction, complexity, part count, mass, volume, and power demand.

The thruster operated in a long-pulse mode with decaying power input converting the potential energy stored in the CDL capacitor bank into kinetic energy. The tested operation of the thruster showed neither instabilities nor problems during the startup sequence and long-pulse discharge mode. The thruster operated along expected characteristics. Namely, anode mass flow rates controlled the discharge current, while magnetic field strength dictated discharge voltage for which efficiency and current were optimized. The CDL/Marx power source produced high energy and power densities with low voltage input. In addition, it demonstrated mass, volume, and part number reduction and powertrain simplification. Two main conclusions can be drawn from the experimental results: First, for the selected operating conditions, the Hall thruster was indifferent to a time-varying voltage input and in fact reproduced performance characteristics similar to previous studies conducted with conventional powertrain architecture. Second, a CDL capacitor bank based and operated on the Marx concept significantly reduces complexity with regard to powertrain configuration as demonstrated in the "nonoptimized" laboratory breadboard unit.

The preliminary mission analysis intended to explore mass benefits and power requirements of electric propulsion and weigh them against a SOA chemical system. Extremes with regard to shading and atmospheric density were chosen to provide a wide spectrum of possible conditions and challenges. Regardless of orbit conditions, all electric propulsion options outperformed the SOA hydrazine monopropellant system in terms of wet mass decrease and

net mass increase. Atmospheric density imposed the greatest challenges with regard to drag compensation and was expected to highlight performance attributes of the propulsion systems. Reduction of necessary onboard power requirement was substantial for capacitor-powered EP options, which directly translates in mass, area, and, most importantly, cost savings. Reduction of dedicated solar array leads to smaller, simpler, and less expensive satellite power generation and conditioning systems. Similar to the experimental goals, a preliminary mission analysis for a very particular near-Earth orbit application lived up to the stipulated objectives. Here, the main conclusion is that the alternate direct-drive option based on a CDL/Marx power source can offer significant benefits with regard to wet and net mass, power, part count, mass, and volume without compromising propulsive performance.

In summary, a Hall thruster (or for that matter any EP thruster) does not really care where the power comes from, or better yet how it is delivered, as long as it is in a form that enables the device to operate. This particular study has shown that this is exactly the case and in doing so is an attractive alternative to powering the thruster. In other words, operating the Hall thruster at distinct voltages, one voltage at a time over a particular voltage operating range (as conducted by Sankovic [26] in an earlier study), is the same as operating the thruster over the same voltage range in a sweeping manner over the course of a few minutes as it occurs with the CDL/Marx power source. Adjusting the mass flow rate as the voltage decreases could compensate the resulting thrust falloff. The attractiveness is that, first, it provides alternative attractive means of powering the thruster, and second, the resulting powertrain offers significant attributes in light of the subsystem and consequently the entire spacecraft and desired mission. Point 1 was demonstrated by the conducted experiments and achieved performance. Point 2 was proven by the mission analysis for a particular selected mission.

Design of a CDL/Marx power source and integration into the powertrain of Hall thruster was successful. Experiments and mission analysis demonstrated clearly the feasibility of an alternate direct-drive EP option for spacecraft applications. The direct-drive, CDL/Marx-powered EP system promises to be a highly efficient, viable alternative for satellite operation in specific near-Earth missions. With this power/propulsion option, power-limited spacecraft can take advantage of efficient, high-specific-impulse, long-life Hall thrusters.

Acknowledgments

The Space Power Institute (SPI) and Center for Commercial Development of Space Power (CCDS) at Auburn University (AU), Alabama, funded this research. The author wishes to thank Steve Best (SPI), M. Frank Rose (Radiance Technologies, Inc.), Rhonald Jenkins (AU), Steve Oleson (NASA John H. Glenn Resarch Center), and Frank Curran (Science Applications International Corporation) for their support and guidance. Further, the author is indebted to the members of the Electric Propulsion Laboratory at NASA John H. Glenn Research Center for their support and assistance, which led to the successful completion of this research.

References

[1] Myers, R. M., "Overview of Major, U.S. Industrial Electric Propulsion Programs," AIAA Paper 2004-3331, July 2004.

[2] Oh, D. Y., "Evaluation of Solar Electric Propulsion Technologies for Discovery Class Missions," AIAA Paper 2005-4270, July 2005.

[3] Woo, B., Coverstone, V. L., Hartmann, J. W., and Cupples, M., "Trajectory and System Analysis for Outer-Planet Solar Electric Propulsion Missions," *Journal of Spacecraft and Rockets*, Vol. 42, No. 3, 2005, pp. 510–516.

[4] Oleson, S., Benson, S., Gefert, L., Patterson, M., and Schreiber, J., "Radioisotope Electric Propulsion for Fast Outer Planetary Orbiters," AIAA Paper 2002-3967, July 2002.

[5] Wong, W. A., Anderson, D. J., Tuttle, K. L., and Tew, R. C., "Status of NASA's Advanced Radioisotope Power Conversion Technology Research and Development," *Proceedings of Space Technology and Applications International Forum (STAIF)*, edited by E.-G. Mohamed, AIP Conference Proceedings 813, American Institute of Physics, Melville, NY, 2006, pp. 340–347.

[6] Guenther, B. D., Weller, H. R., and Godwin, J. L., "Search for Nuclear Isotopes for Use in a Nuclear Battery," *Journal of Propulsion and Power*, Vol. 17, No. 3, 2001, pp. 540–546.

[7] Joyner, C. R., Fowler, B., and Matthews, J., "A Closed Brayton Power Conversion Unit Concept for Nuclear Electric Propulsion for Deep Space Missions," *Proceedings of Space Technology and Applications International Forum (STAIF)*, edited by E.-G. Mohamed, AIP Conference Proceedings 654, American Institute of Physics, Melville, NY, 2003, pp. 677–684.

[8] Bennett, G. L., Hemler, R. J., and Schock, A., "Space Nuclear Power-An Overview," *Journal of Propulsion and Power*, Vol. 12, No. 5, 1995, pp. 901–910.

[9] Casani, E. K., and Wilson, B. W., "The New Millennium Program: Technology Development for the 21st Century," AIAA Paper 96-0696, Jan. 1996.

[10] Hamley, J. A., Sankovic, J. M., Lynn, P., O'Neill, M. J., and Oleson, S. R., "Hall Thruster Direct Drive Demonstration," AIAA Paper 1997-2787, July 1997.

[11] Hoskins, W. A., Homiak, D., Cassady, R. J., Kerslake, T., Peterson, T., Ferguson, D., Snyder, D., Mikellides, I., Jongeward, G., Schneider, T., and Hovater, M., "Direct-Drive Hall Thruster System Development," AIAA Paper 2003-4726, July 2003.

[12] Schneider, T., Mikellides, I. G., Jongeward, G. A., Peterson, T., Kerslake, T. W., Snyder, D., and Ferguson, D., "Solar Arrays for Direct-Drive Electric Propulsion: Arcing at High Voltage," *Journal of Spacecraft and Rockets*, Vol. 42, No. 3, 2005, pp. 543–549.

[13] von Helmholtz, H. L. F., "Über einige Gesetze der Verteilung elektrischer Ströme in körperlichen Leitern," *Annalen der Physik und Chemie*, Vol. 89, 1853, pp. 211–233.

[14] Brett, C. M. A., and Brett, A. M. O., *Electrochemistry: Principles, Methods, and Applications*, Oxford Univ. Press, New York, 1993.

[15] Murphy, O. J., Srinivasan, S., and Conway, B. E., *Electrochemistry in Transition-From the 20th to the 21st Century*, Plenum Press, New York, 1992.

[16] Merryman, S. A., and Hall, D. K., "Chemical Double-Layer Capacitor Power Source for Electromechanical Thrust Vector Control Actuator," *Journal of Propulsion and Power*, Vol. 12, No. 1, 1996, pp. 89–94.

[17] Bockris, J. O'M., "Overview of the Current Status of Solid-Liquid Interface Science," *Materials Science and Engineering*, Vol. 53, No. 1, April 1982, pp. 47–64.

[18] von Helmholtz, H. L. F., "Studien über elektrische Grenzschichten," *Annalen der Physik und Chemie*, Vol. 7, 1879, pp. 337–382.

[19] Rose, M. F., "Performance Characteristics of Large Surface Area Chemical Double Layer Capacitors," *Proceedings of the 33rd International Power Source Symposium*, The Electrochemical Society, Penningham, NJ, 1988, pp. 572–592.

[20] Rose, M. F., Johnson, C., Owens, T., and Stephens, B., "Limiting Factors for Carbon-Based Chemical Double-Layer Capacitors," *Journal of Power Sources*, Vol. 47, No. 3, Jan. 1994, pp. 303–312.

[21] Kurzweil, P., and Schmid, O., "High Performance Metal Oxide Supercapacitors," *Proceedings of the 6th International Seminar on Double Layer Capacitors and Similar Energy Storage Devices*, Florida Educational Seminars, Deerfield Beach, FL, 1996.

[22] Zheng, J. P., Cygan, P. J., and Jaw, T. R., "Hydrous Ruthenium Oxide as an Electrode Material for Electrochemical Capacitors," *Journal of the Electrochemical Society*, Vol. 142, No. 8, 1995, pp. 2699–2703.

[23] Rose, M. F., Lai, J., and Levy, S., "High Energy Density Double-Layer Capacitors for Energy Storage Applications," *IEEE Aerospace and Electronics Systems Magazine*, Vol. 7, No. 4, 1992, pp. 14–19.

[24] Kurzweil, P., and Dietrich, G., "Double Layer Capacitors for Energy Storage Devices in Space Applications," *Proceedings of the 2nd International Seminar on Double Layer Capacitors and Similar Energy Storage Devices*, Florida Educational Seminars, Deerfield Beach, FL, 1992.

[25] Yoshida, A., Nishino, A., and Ohara, K., "Electric Double-Layer Capacitors for High Rate Charge-Discharge Uses," *Proceedings of the 2nd International Seminar on Double Layer Capacitors and Similar Energy Storage Devices*, Florida Educational Seminars, Deerfield Beach, FL, 1992.

[26] Sankovic, J. M., and Haag, T. W., "Operation Characteristics of the Russian D-55 Thruster with Anode Layer," NASA TM-106610, 1994.

[27] Sankovic, J. M., Hamley, J. A., and Haag, T. W., "Performance Evaluation of the Russian SPT-100 Thruster at NASA LeRC," NASA TM-106401, 1994.

[28] Garner, C. E., Brophy, J. R., Polk, J. E., Semenkin, S., Garushka, V., Tverdokhlelov, S., and Marrese, C., "Experimental Evaluation of a Russian Anode Layer Thruster," AIAA Paper 1994-3010, June 1994.

[29] Hrbud, I., and Rose, M. F., "Direct-Drive Concept Based on CDL

Capacitor Technology Powering a Thruster with Anode Layer," AIAA 97-1007, Jan. 1997.
[30] Hrbud, I., "Evaluation of Performance and Characteristics of Long Pulse Hall-Ion Thrusters Utilizing a Power Source Based on CDL Capacitor Technology," Ph.D. Dissertation, Auburn University, Auburn, AL, 1997.
[31] Hrbud, I., Rose, M. F., and Merryman, S. A., "A Simple Marx Power System for Pulsed Plasma Thrusters," IEPC Paper 97-123, Aug. 1997.
[32] Patterson, M. J., Haag, T. W., Rawlin, V. K., and Kussmaul, M. T., "NASA 30-cm Ion Thruster Development Status," NASA TM 106842, 1994.
[33] Hamley, J. A., and Patterson, M. J., "Integration Testing of the Space Station Plasma Contactor Power Electronics Unit," AIAA Paper 94-3307, June 1994.
[34] Oleson, S., and Sankovic, J. M., "Benefits of Low Power Electrothermal Propulsion," NASA TM-107404, 1996.
[35] Campbell, R. E., Browell, E. V., Ismail, S., Dudelzak, A. E., Carswell, A. I., and Ulitsky, A., "Feasibility Study for a Spaceborne Ozone/Aerosol Lidar System," *Proceedings of the 18th International Laser Radar Conference (ILRC)*, Springer–Verlag, Berlin, July 1996.
[36] Browell, E. V., Fenn, M. A., Butler, C. F., Grant, W. B., Clayton, M. B., Fishman, J., Bachmeier, A. S., Anderson, B. E., Gregory, G. L., Fuelberg, H. E., Bradshaw, J. D., Sandholm, S. T., Blake, D. R., Heikes, B. G., Sachse, G. W., Singh, H. B., and Talbot R. W., "Ozone and Aerosol Distribution and Air Mass Characteristics over the South Atlantic Basin During the Burning Season," *Journal of Geophysical Research*, Vol. 101, 1996, pp. 24,043–24,068.
[37] Hrbud, I., Rose, M. F., Oleson, S. R., and Jenkins, R. M., "TAL Performance and Mission Analysis in a CDL Capacitor Powered Direct-Drive Configuration," AIAA Paper 97-2786, July 1997.

G. Spanjers
Associate Editor